Israel Journal of Chemistry

DOI: 10.1002/ijch.201300017

Photoswitching Emission with Rhodamine Spiroamides for Super-resolution Fluorescence nanoscopies

Vladimir N. Belov[a] and Mariano L. Bossi*[b]

Abstract: Spatial resolution in far-field fluorescence microscopy is limited by diffraction to about 200 nm. With the aid of photoswitchable fluorophores, the diffraction barrier has been successfully overcome, allowing unprecedented resolution in the order of single biomolecules. The imaging process demands markers with strict and reliable control of the switching, to keep most of the markers in a non-emissive state most of the time and to bring a tiny number back to an emissive state, and detection at the single-molecule level. Herein, we describe the use of rhodamine spiroamides with unique photophysical properties as molecular probes for super-resolution techniques based on the localization of single emitters. This family of photochromic and fluorescent compounds fulfils the stringent requirements for such imaging methods; these compounds are robust and capable of enduring single-molecule detection in diverse environments. This has allowed meaningful images with resolution down to a few nanometres. Their design, synthesis and implementation is discussed along with imaging applications in material and life sciences.

Keywords: fluorescence · optical nanoscopy · photochemistry · photochromism

1 Introduction

Fluorescence microscopy represents a milestone in life sciences research. It offers unparalleled advantages, such as simple sample preparation, 3D rendering, non-invasive character and compatibility with live-specimen observation. However, the low spatial resolution is not always sufficient to elucidate organelles or subcellular structures. This limit in resolution arises because far-field microscopes rely on focusing light with conventional lenses that act as apertures in the beam path, inevitably resulting in a diffraction phenomenon. As a consequence, features that are closer than about 200 nm remain unresolved. The "diffraction barrier" was overcome by a revolutionary idea:[1] the use of two molecular states of the fluorescent probe; a bright (fluorescent) state and a non-emissive (dark) one. This idea gave rise to several different techniques, for example, stimulated emission depletion (STED) microscopy,[1a] reversible saturable optical fluorescence transmission (RESOLFT) microscopy,[2] photoactivated localized microscopy (PALM),[3] stochastic optical reconstruction microscopy (STORM),[4] and ground-state depletion microscopy (GSDIM).[5] Photoswitching between these two states is the main feature in all modern far-field super-resolution microscopies, and this switching can be done either in a targeted[1a,2,6] or in a stochastic fashion.[3–5,7] Recently, stochastic methods have become very popular due to the simplicity of the required setup. The imaging process is shown schematically in Figure 1.[4,7a,8]

At the beginning of any given measurement, all markers should be either in, or switched to, the dark state. Single emitters are then switched on in random positions and imaged with a charge-coupled device (CCD) camera in a wide-field illuminated microscope. Diffraction makes them appear in the image as blurred spots of about 200 nm. Therefore, each frame is still diffraction limited and only a small and sparse subset of fluorescent markers must be in the bright state to be resolved from their neighbours (i.e., separation between markers should be ca. 5-fold the resolving power of the microscope). If this condition is fulfilled, the position of each fluorophore can be pinpointed with an improved accuracy factor of about $1/\sqrt{N_{PH}}$, in which N_{PH} is the number of detected photons.[9] Before the next frame can be recorded, these markers have to return to (or be enforced to) the dark state again and a new subset is then switched on. This

[a] V. N. Belov
Department of NanoBiophotonics
Max Planck Institute for Biophysical Chemistry
Am Fassberg 11
37077 Göttingen (Germany)

[b] M. L. Bossi
INQUIMAE and Departamento de Química Inorgánica, Analítica y Química Física
Facultad de Ciencias Exactas y Naturales
Universidad de Buenos Aires, Pabellón 2
Ciudad Universitaria, 1428 Buenos Aires (Argentina)
e-mail: mariano@qi.fcen.uba.ar

process is repeated over and over again, so that thousands of frames are acquired. Software analysis renders a list of the positions of the multitude of detected markers. Their 2D mapping produces an image, the spatial resolution of which converges to the average sub-diffraction localization accuracy.

The equipment required is simply a conventional wide-field microscope with single-molecule (SM) detection capability, that is, with highly efficient photon collection and detection (a high aperture immersion objective lens; low number of high-end optical components, filters, lenses, etc.; and laser excitation). Thus, the fluorescent marker in such setups is very important because it is responsible for the success in converting a diffraction-limited measurement to a diffraction-unlimited one. Additionally, its performance directly translates into the achievable spatial resolution and quality of the images. Although reversibility is not strictly required, and irreversibly photoactivatable fluorophores are useful too (switching off is addressed by photobleaching), reversible systems are advantageous because they afford several activation/deactivation cycles per molecule. In fact, reversible markers are predominant in the literature.[10]

Photochromic dyes, with their two photoisomers as the bright and dark states, are particularly appealing for stochastic super-resolution microscopies. The importance of the probe comes in line with the requirement for outstanding performance under harsh conditions in SM observation. A number of well-defined photophysical and photochemical properties is necessary. Firstly, as stated before, photoswitching between an emissive and a non-emissive state is mandatory. Secondly, fluorescence and photochromism of the label are simultaneously required. Thirdly, tight control of the switch-on and -off processes is also important to shift the equilibrium virtually to com-

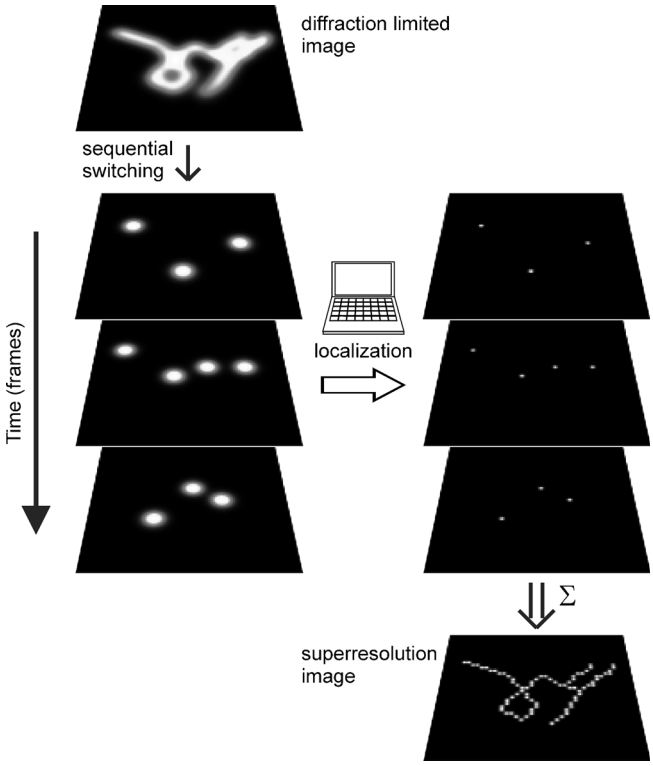

Figure 1. Stochastic super-resolution imaging process. If all markers are switched on, a diffraction limited image is obtained (top left); therefore, they should be switched off before the process is started. In every frame (left series) only a few markers are in the bright state (the rest are switched off) and this population is renewed in each successive frame. For proper localization, bright markers have to be sparsely distributed. This localization renders a list of positions (right-hand series); a 2D mapping of them results in an image with resolution determined by the average localization accuracy (bottom right).

Mariano L. Bossi studied chemistry at the University of Buenos Aires (UBA), Argentina, where he received his MS in Chemistry in 1998, and a PhD degree in Physical Chemistry in 2003. From 2004 to 2008, he was a post-doctoral researcher at the Max Planck Institute for Biophysical Chemistry, Department of NanoBiophotonics (Göttingen, Germany), and a Marie Curie Fellow, implementing bistable photochromic compounds into modern fluorescence nanoscopies. In 2008, he was appointed as a member of the research staff of the Consejo Nacional de Investigaciones Científicas y Técnicas (CONICET), working at the Institute of Physical Chemistry of Materials, Environment and Energy (INQUIMAE). In 2009, he was appointed Professor at the School of Sciences (FCEN) of the UBA. On his return to Argentina, he founded the Photonic Nanoscopies Laboratory, an experimental research group at Inquimae-UBA. His current research interest is centred on the development of fluorescent switchable probes for super-resolution microscopy.

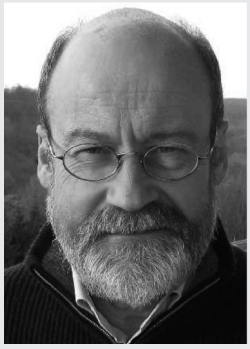

Vladimir N. Belov studied chemistry at Leningrad State University (Russia), where he obtained his doctoral degree in 1985 under the supervision of Prof. M. A. Kuznetsov. In 1985–1993, he held various positions at the chairs of organic, physical organic and natural product chemistry at the Chemistry Department of Leningrad (St. Petersburg) University. In 1993, he joined the group of Prof. A. de Meijere (Georg-August-Universität Göttingen, Germany). Later he worked as a post-doctoral researcher for BASF and BAYER and was engaged in several contract research and custom synthesis projects for Procter & Gamble (in Russia) and KAdem Custom Chem GmbH (2000–2005, Göttingen). In 2005, he became a group leader at the Department of NanoBiophotonics founded by Prof. S. W. Hell at the Max Planck Institute for Biophysical Chemistry (Göttingen). His current research interests focus on the chemistry of organic fluorescent compounds.

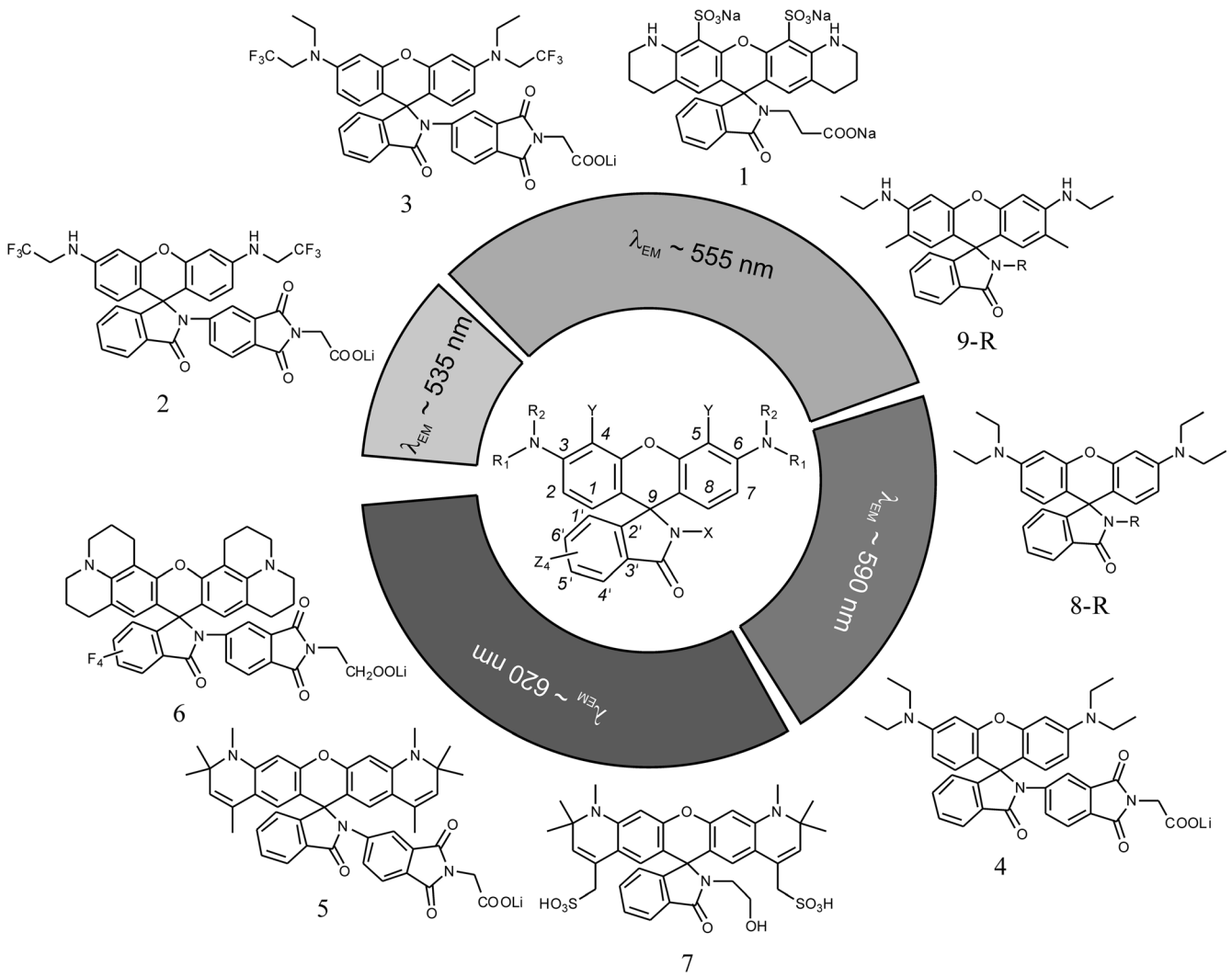

Scheme 1. Chemical structures of some RSAs prepared, sorted by emission wavelength.

plete conversion towards the dark form. Importantly, the quality of the final image scales up with the amount of detected markers, that is, with the number of markers present (labelling density). However, the number of labels in the bright state at any time is practically fixed by the field of view. Therefore, if the labelling becomes denser, the equilibrium should be even more shifted towards the dark isomer. This asymmetry in the equilibrium indicates that the signal of the isomer in the bright state has to be several orders of magnitude higher than that of the "dark" one. Isomers with bright/dark ratios of 20 : 1 to 100 : 1, which perform more than satisfactorily in ensemble applications, perform poorly in such stochastic approaches. Finally, detection at the SM level is needed, and therefore, the brightness and photoresistance of the "bright" isomer play a key role because they directly influence the spatial resolution. Additionally, there are other relevant factors in the design of a useful photoswitch. A 10-fold resolution improvement requires at least 100 detected photons (per marker) in a frame of typically 10 ms; thus, photons must be emitted efficiently and in a short time. That is, not only the emissive excited state (of the "bright" isomer) should exhibit a large quantum yield, but it should also be short-lived (i.e., fluorescence – not phosphorescence – is required as the emission process).

A large number of fluorescent molecular switches based on a molecular assembly composed of a photochromic and a fluorescent building block is described in the literature,[11] but only a few are suitable for SM detection.[12] A predominant fraction of them relies on an emission-modulation mechanism based on the excited-state resonant energy transfer from the fluorophore to one of the isomers of the photochrome.[13] Such a mechanism suffers from an erasing effect (an undesired bright-to-dark-state conversion) while reading the signal. Erasing prevents their detection at the SM level, unless the reaction responsible for erasure is very inefficient.[14] An alter-

native is the use of fluorescent switches where the bright-to-dark-state isomerization can only proceed through a thermal path (via ground states), or the changes in the emission properties rely on ground-state changes (e.g., a bathochromic shift of the fluorophore absorption)[15] rather than on excited-state processes. Thus, competition between the two key processes, emission and isomerization, is no longer a problem. Rhodamine spiroamides (RSAs, Scheme 1) belong to a family of fluorescent photoswitches, the modulation of which is not based on excited-state processes. Moreover, they meet all requirements for fluorescence nanoscopies based on photoswitching and the localization of single emitters. Herein, we summarize their use as extrinsic markers (non-genetically encoded probes) in such techniques, along with their main relevant properties.

2 Photochromism of RSAs

RSAs (Figure 2) belong to a family of photochromic compounds, the fluorescence properties of which differ from most of the known photochromes (azobenzenes, diarylethenes, fulgides, spiropyranes, etc.). One of their isomers is highly fluorescent (typically with $\Phi_{Fluo} > 0.5$) in chlorinated solvents, toluene, acetonitrile, alcohols, and even in aqueous media. Moreover, photochromic behaviour is conserved in solid or viscous environments, such as silica gel or polymeric films (e.g., PVA, poly(methyl methacrylate) (PMMA)).[16–18]

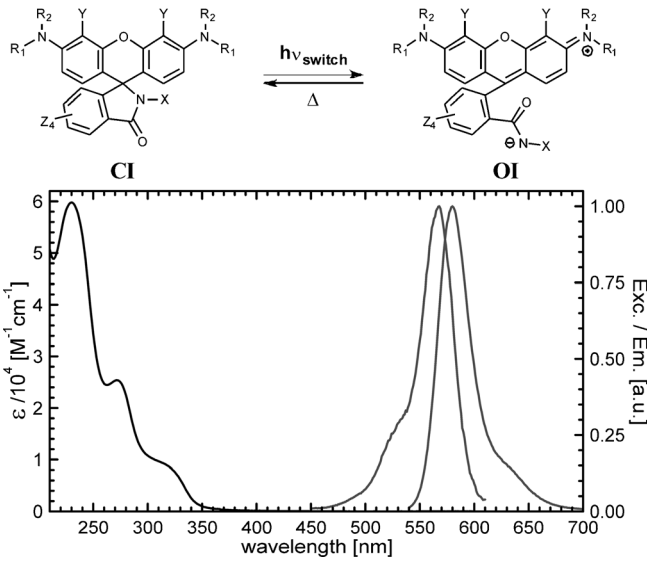

Figure 2. Photochromism of RSAs. Photoswitching of the "closed" isomer (CI, black line) with UV light produced an "open" isomer (OI, grey lines) with absorption and emission properties of a rhodamine. The spectra shown correspond to compound **4** (in Scheme 1) with $R^1 = R^2 = Et$, $Y = Z = H$, and $X = [N\text{-(carboxymethyl)phthalimid}]\text{-3-yl}$ in a polyvinyl alcohol (PVA) film. Adapted with permission from reference [16].

RSAs are formed from the free carboxyl group at the 3'-position of a rhodamine in the course of amidation with an aromatic or aliphatic primary amine followed by intramolecular cyclization to a five-membered spirolactam ring. The latter is the thermally stable isomer (closed isomer, CI) of the photochromic system. Cyclization breaks the extended conjugation in the rhodamine chromophore and removes the positive charge from the xanthene fragment, resulting in the disappearance of its characteristic absorption and emission in the visible range. The CI shows a typical pattern of three bands in the UV, one of which is at around 310–340 nm (depending on the substitution pattern) and is responsible for photochromism. Irradiation at these wavelengths breaks the C(9)–N spiro bond, restoring the rhodamine chromophore, and is followed by a protonation of the negatively charged amide residue. Switching efficiencies, that is, isomerization quantum yields, are very low, in particular, in aqueous or polar solvents.[19] The metastable open isomer (OI) retains the emission properties of the initial rhodamine. Remarkably, the back reaction is the nucleophilic attack of the amide nitrogen and thus proceeds from the ground state through a thermal pathway. As a result, the lifetime of the OI strongly depends on the environment, ranging from milliseconds to hundreds of seconds.[19,20] Irradiation in the visible band of the OI exclusively and with high efficiency results in fluorescence emission. The excited state is localized on the condensed-ring system. Apparently, it barely modifies the nucleo- and electrophilic properties of the respective atoms responsible for back isomerization.

The photophysical properties of RSAs limit their use in some common applications of photochromic compounds.[21] For example, few or no compounds of this family are found in applications such as optical information storage, phototriggered phase transitions or refractive index changes. One possible reason is the poor ring-opening quantum yield, which results in very low conversion to the OI in the photostationary state. Nevertheless, this two-state system fits the requirements for switchable probes for fluorescence nanoscopy perfectly: i) the thermally stable isomer is the dark state in the image recording scheme; ii) virtually infinite signal contrast is achieved both at the ensemble level, because the fraction of molecules in the OI in thermal equilibrium (in a non-illuminated sample) is negligible, and at the molecular level, because the absorption of the CI in the visible is virtually zero; iii) the absence of the erasing effect allows the interrogation of the system at such probing-light intensities (close to saturation excitation intensities, in the absorption band of the OI) that they allow the extraction of the largest amount of photons in the shortest possible time, provide fast overall imaging times, and precisions down to the macromolecular level; iv) the fluorophore presents outstanding photostability, in fact, it has been widely used as fluorescent markers in biological systems and in SM

experiments;[22] and v) the poor activation (ring-opening) quantum yield is actually an advantage for this particular purpose, facilitating maintenance of the sparse population fraction in the OI.

Although any control of the OI lifetime is unattainable with light, it lies within the required timeframes for optical measurements, at least in aqueous media. Thus, it allows measuring at the fastest recording schemes attainable, by adjusting the frame rate to the average rate of the conversion between the emissive and dark states.[23] Fortunately, a light source for switching off the bright state of a RSA (i.e., a refreshing process between frames) is unnecessary, resulting in a simpler and more economic setup. In addition to these advantages, the preparation of RSAs is relatively simple and well established. In fact, some markers can be prepared from commercially available and inexpensive rhodamines in a few synthetic steps (see Section 5).

3 Halochromism of RSAs

In addition to a response to light stimuli, RSAs are also responsive to changes in the proton concentration (Figure 3). This makes RSAs potential fluorescence pH indicators, with fluorescence switching on at low pH,[24] due to a strongly coloured protonated isomer (OI–H^+). The OI may even be detected with the naked eye, as a result of the large absorption coefficient of rhodamine chromophores (10^4–10^5 M^{-1} cm^{-1}). The K_a values are in the range of 10^{-3}–10^{-5},[20,25] but the thermal equilibrium after the addition of acid is reached in seconds (it is faster in aqueous solutions) and follows a linear dependence with proton concentration.[20] This relatively slow equilibration may limit the utility of RSAs as proton sensors in applications where a fast response is necessary.

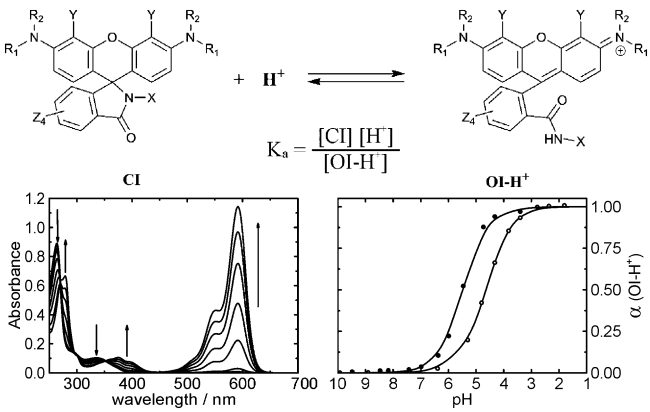

Figure 3. Halochromism of RSAs (top). pH-induced changes in the absorption of compound **7** in buffered solutions (bottom left). Speciation diagram (bottom right) for compounds **5** (filled circles) and **7** (hollow circles). Adapted with permission from reference [25].

The stable form in acidic solution is identical to the OI obtained in the course of the photochromic ring-opening process followed by proton addition and so are their photophysical properties. Therefore, most of the ensemble properties (absorption and emission spectra, fluorescence lifetime, fluorescence quantum yield) of bright isomers were measured in acidified solution. When it was possible to compare an OI obtained upon acidification and by photolysis (for example, in polymer films where the lifetime of the OI is long), no difference was found.

In a similar manner, the proton-like response can be extended to other cations, if one or more electron-donating heteroatoms are present near the lactam nitrogen. In this case, an open adduct is formed with the lactam/amide nitrogen and the other donors chelating the metallic analyte. This idea has been extensively exploited for the design of RSA chemosensors with a switch-on response to Hg^{2+}, Zn^{2+}, Fe^{3+}, Pb^{2+}, and so forth.[26] Another working principle was also reported.[27] A 1,2-bis(*o*-aminophenoxy)ethane-*N*,*N*,*N*′,*N*′-tetraacetic acid (BAPTA) chelator at positions 2 and 3 of the xanthene chromophore (for numbering, see Scheme 1) only has a high affinity to Ca^{2+} ($K_d \approx 500$ nM) in the CI; in the OI, the nitrogen atom is positively charged and the complexation ability becomes very poor ($K_d \approx 180$ μM). This results in a chemosensor, the calcium affinity of which can be modulated with light.

The response of all RSAs prepared so far occurs at a pH below biologically relevant values (typically, pH = 7.4). Thus, heliochromism does not interfere with photoswitching when RSAs are used as fluorescent markers in SM localization nanoscopies. Nevertheless, in acidic solvents, or when the RSA marker occupies a position near to proton-donating groups, imaging with super-resolution may be precluded. In these cases, the probe becomes a standard fluorescent rhodamine dye and imaging in conventional mode (i.e., wide-field or confocal) with diffraction-limited resolution are still possible.

4 Fluorescence Emission and Switching Properties

The chemical structure of the metastable OI represents a 3'-carboxamido derivative of a typical rhodamine dye (eventually bearing an additional free carboxylic group; Figures 2 and 3). Similar amides with a fixed OI can be prepared from secondary amines. Such compounds were reported to have similar photophysical properties to those of the parent rhodamines.[28,29] In fact, some commercial labels represent these kinds of rhodamine derivatives, usually with *N*-methyl residues and a longer chain with a reactive group (e.g., succinimidyl ester) at the other terminus of an *N*-alkyl chain.[30] Analogously, the photophysical properties of the OIs are also similar to those of the parent rhodamine. As a rule of thumb, substitution provides a 5–10 nm redshift of the absorption

and emission peaks of the visible band (with respect to the parent rhodamine with a free carboxylic acid group), and the fluorescence lifetime and quantum yield are barely altered. For example, lifetimes are in the range of 2–4 ns and quantum yields are reduced no more than to 10%. As a result, the emission properties of the desired RSA switch are determined and can be tuned by the selection of a parent rhodamine. The choice is usually influenced in terms of the particular imaging application or equipment available (laser sources, filter cubes, etc.). The same applies to the selection of dyes for multicolour applications.[17,25]

Despite the low switching efficiency of RSAs and the fact that photoactivation is performed at the side of the absorption band (sometimes with very marginal absorption), measurements at the SM level established that low activation intensities were efficient enough to maintain the sparse population of emitters required for localization microscopies. Optimal values depend on each particular marker and sample, but in general low activation intensities were used, in the range of tens of W cm^{-2} at 375 nm. The wavelength is of particular importance for live imaging applications; shorter wavelengths should be avoided because of cell damage. Nevertheless, the activating UV light should not irradiate the sample continuously. Typically, a short pulse (<500 μs) was applied between two successive frames, when the CCD camera was being read.

There are two factors that define the wavelength of the activation light. The first one is instrumental: on one hand, the availability of reliable lasers with enough power and a good output mode in the range of wavelengths where the RSAs present a sufficient absorption is rather limited; on the other hand, light transmission of optical components below about 350 nm is seriously compromised, in particular, for objective lenses. The second factor is related to the absorption coefficients of the CI. In this respect, chemical modification resulted in a required redshift of the band that contributed to the absorption at the wavelength of the available laser sources, for example, 355 and 375 nm.

Although it is not a universal and general rule, we found that the most effective spectral shifts were achieved with modifications introduced into the rhodamine part rather than into the amine residue (Figure 4). These

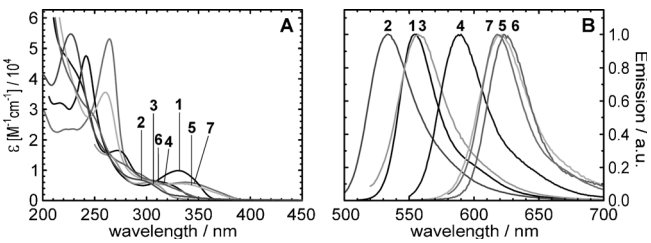

Figure 4. Absorption (A) and emission (B) spectra of compounds **1**–**7** in Scheme 1. Adapted with permission from reference [25].

structural modifications also shift the bands in the absorption and emission spectra of the "bright" isomer. Therefore, it is sometimes difficult to independently adjust the absorption spectra of both isomers. In general, changes in the positions of the absorption maxima of the OI are more pronounced than changes in the positions of the long-wavelength band of CI. For example, the structurally similar alkyl derivatives of rhodamine B and 6G (8-cyclohexyl/9-cyclohexyl or 8-Me and 9-Me)[20] have a peak absorption difference of 15 nm for the CIs and 25 nm for the OIs (with both isomers of the rhodamine 6G adduct absorbing at shorter wavelengths). Exceptions were encountered in some cases when electron-withdrawing substituents were attached to C3/C6 amino groups (CF_3CH_2 in compounds **2** and **3**) or present in the phenyl ring bearing the carboxyl acid group of the rhodamine (as in compound **6**). In the former case, these groups produce a blueshift of about 30 nm in the absorption of the respective CI, but have little effect on the absorption and emission of the OIs (compare compounds **1** and **3**, or compound **6** with **5** and **7** in Table 1). On the contrary, sulfonate groups at C4 and C5 produce an important bathochromic shift of the CI absorption, with little effect on the absorption and emission properties of the other isomer (compound **1**).

A particular case was found for compound **7**. It was designed as a red emitter (620 nm), by the addition of two double bounds to extend the conjugation in the chromophore. This compound has a rigid xanthene fragment, which is known to increase its photostability.[31] However, we observed that, after prolonged imaging times (under combined irradiation with 375 nm activation and high-intensity 532 nm excitation), blueshifting of the emission to about 580–590 nm was induced. The reason for this effect could be (stepwise) photoinduced oxidation of the two additional double bonds by atmospheric oxygen to yield products with simple C–C bonds (instead of double bonds). This phenomenon is of particular importance in prolonged imaging experiments; it can cause a time-dependent reduction in collected photons, and thus, a reduction in the average spatial resolution or even false assignment of single markers in multicolour imaging.[17] Alternatively, a red-emitting RSA was prepared by using tetrafluorophthalic anhydride, which led to the perfluorinated aromatic ring attached to C9 of the xanthene residue in compound **6**. Its emission peak is at 625 nm and it is more photostable than compound **7**, yields more photons per frame under similar SM imaging conditions, and no colour shift is observed. The drawback is that this marker is far more lipophilic and very poorly soluble in water. This property was only partially compensated for by the incorporation of hydrophilic residues in the reactive group.

The substituent attached to the lactam nitrogen plays a minor role in shifting the absorption of either isomer.[20,25,32] For example, rhodamine B analogues with

either *N*-benzene or *N*-cyclohexane rings (8-phenyl and 8-cyclohexyl) have absorption peaks at exactly the same wavelengths for both isomers.[20] A similar conclusion can be drawn from a comparison between compounds **5** and **7**.[25,32] However, aromatic groups at this position appear to increase the activation efficiency either by weakening the C(9)–N bond through inductive or mesomeric effects, or by stabilizing the negative charge that initially forms on the amide nitrogen upon breaking the C(9)–N bond.

RSAs present an interesting property, which is rare in other families of common probes in SM-based super-resolution microscopies. Switching on the fluorescence signal through a two-photon absorption process is possible with available instruments, that is, under conditions similar to those of the conventional two-photon fluorescence microscopes. Activation is then performed with far-red wavelengths (647–750 nm). In comparison with UV light, long wavelengths minimize potential cell damage and have more penetration depth due to lower absorption and light scattering. Excitation with two photons also endows the technique with a unique advantage: optical sectioning. The quadratic dependence of the efficiency of this process limits switching to markers that are near to the focal plane. The thickness of that "active" layer is >600 nm[33] and the resolution in the axial direction remains diffraction limited. Nevertheless, there is a substantial improvement with respect to one-photon activation, because thick samples can be imaged, and total internal reflection (TIRF) recording schemes or mechanical object slicing are not mandatory. In addition, super-resolution imaging can be performed at different focal planes. The result is a 3D rendering similar to the one obtained in a confocal or a two-photon microscope (*z* stack), but where every stack has sub-diffraction resolution. Out of focus markers are not subjected to switching and excitation; therefore, they are not bleached, their population remains unaltered, and the quality and resolution within each stack is similar and independent from the order in which they are recorded (provided that other conditions are similar too). It was proved that images obtained with one- and two-photon switching processes were virtually indistinguishable (Figure 5). Furthermore, excellent *z* stacks were obtained with different RSA markers (Section 6.3). In fact, RSAs were the first fluorophores that allowed imaging with thick samples and 3D image rendering.

The drawback of two-photon activation is that it is usually performed with short (picosecond) pulses and high intensities.[16] A more expensive, mode-locked titanium-sapphire laser and a beam scanner for this source are needed; this increases the price and complexity of the experimental setup. Later it was demonstrated that two-photon activation of RSAs was also possible with simpler and cost-effective continuous-wave (CW) lasers.[32] Chemical design of the marker allowed the two-photon absorption to be increased, by extending the conjugation within the rhodamine chromophore (Figure 5). These modifications resulted in a redshift in the absorption of both isomers.

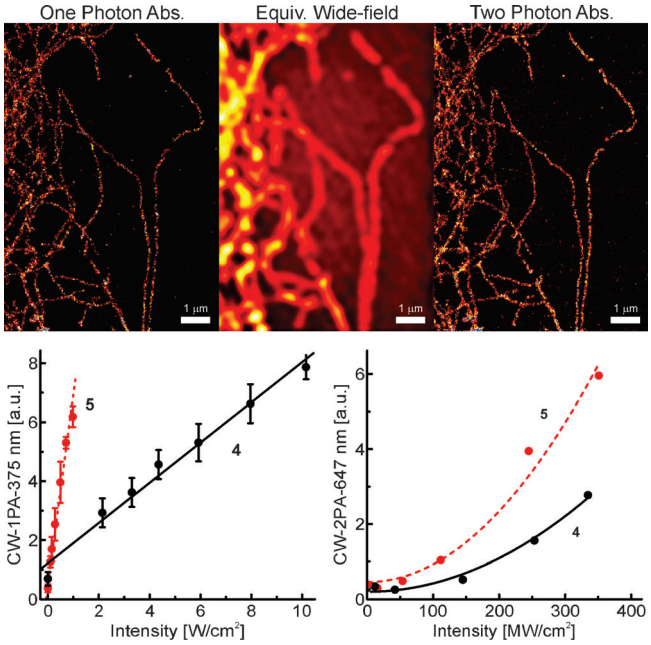

Figure 5. Top: Super-resolution images of a tubulin network of a PtK2 cell, with compound **4**-NHSS (*N*-hydroxy(sulfosuccinimidyl) ester). Photoswitching was performed through one- (375 nm) or two-photon absorption (747 nm, pulsed) processes; the wide-field image is shown in the centre (all frames added). Bottom: Intensity dependence of the photoinduced ring-opening reaction of compounds **4** and **5** in 40 nm thick PVA films containing identical amounts of the corresponding dye. One-photon photoswitching was performed at 375 nm (left) and two-photon photoswitching with a CW laser at 647 nm (right). Adapted with permission from references [16] and [32].

Super-resolution techniques based on the localization of single emitters have been recently extended to allow sub-diffraction resolution in 3D (i.e., also in the axial direction). Different implementations that undoubtedly increase the complexity of the technique are possible, such as astigmatic detection,[34] bifocal imaging,[35] and interferometric detection.[36] RSAs were already applied in two of those approaches with excellent results[18,37] (Section 6.3).

5 Synthesis of RSA Markers

5.1 Formation of the Amide (Lactam) Bond

The most general route we used to prepare RSAs was based on the activation of the carboxylic acid group in a rhodamine dye (Scheme 2) with $POCl_3$. After removal of $POCl_3$ and changing the solvent, the acid chloride reacted with the desired amine and formed the required RSA. (Remarkably, acylation of diazomethane with rhodamine acid chlorides followed by spontaneous cyclization

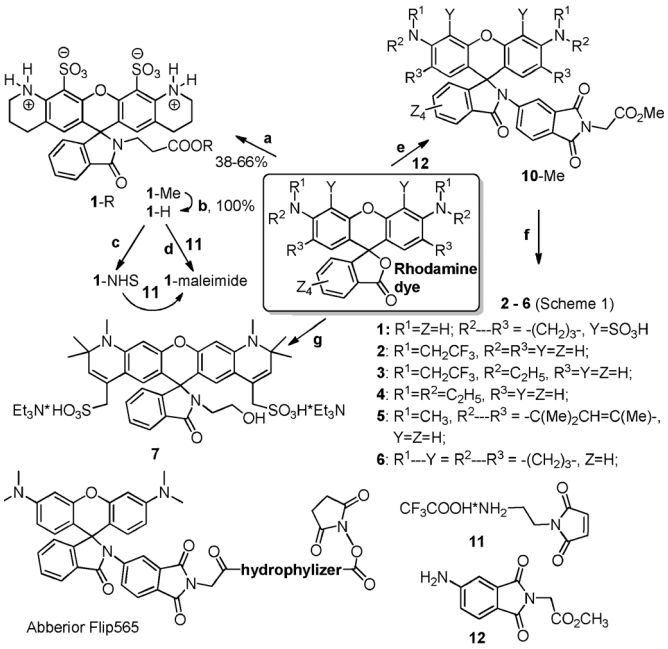

Scheme 2. Main synthetic routes used for the preparation of RSAs: a) *N,N,N′,N′*-tetramethyl-*O*-(*N*-succinimidyl)uronium tetrafluoroborate (TSTU), Et_3N, DMF, RT, overnight; HCl–$H_2NCH_2CH_2COOMe$, Et_3N, DMF, RT, overnight; b) 0.1–0.15 M aq. NaOH, RT, 2 h; c) Amberlite IR-120 (H^+ form), then TSTU, Et_3N, DMF, 0°; d) *O*-(7-azabenzotriazol-1-yl)-*N,N,N′,N′*-tetramethyluronium hexafluorophosphate (HATU), DMF, RT, overnight; e) $POCl_3$, $ClCH_2CH_2Cl$, reflux; CH_3CN, **12**, Et_3N, RT; f) LiI, THF, reflux 3–4 d; g) $H_2N(CH_2CH_2)OH$, HATU; then *N,N′*-di(succinimidyl) carbonate, CH_3CN/DMF, Et_3N, RT −40°. NHS = *N*-hydroxysuccinimidyl.

to spiro 2-diazoketones is also possible.[38]) For example, compounds **2**–**6** and **8**-phenyl were prepared by this route. In most practically relevant cases, we used 3-amino-*N*-(methoxycarbonylmethyl)phthalimide (**12**; Scheme 2) as an amine. It served as a "light antenna" and contained the (protected) carboxyl group required for bioconjugation. It also provides the required absorption (i.e., a small shoulder or foot in the red edge of the band at $\lambda > 340$ nm; Figure 2) in compounds **2**–**6**, so that they can be photoactivated with 375 nm laser light or, in two-photon mode, with 647 nm light.

Unfortunately, this synthetic approach has limitations. First of all, in most cases, it is inapplicable to rhodamines with primary and secondary amino groups (e.g., rhodamines 110 and 6G) because these amines react with $POCl_3$ and may be acylated with acid chlorides. However, if the amino group bears a one-electron acceptor, such as 2,2,2-trifluoroethyl substituent (like in compound **2**), the corresponding rhodamine may be converted into an acid chloride and RSA because *N*-(2,2,2-trifluoroethyl)amino groups do not react with $POCl_3$ and do not easily undergo acylation with aryloyl chlorides. The zwitterionic rhodamines in the open form bear a positive charge localized mostly on the nitrogen atoms and, to some extent, in the xanthene fragment. On the contrary, RSAs lack this charge, and thus, the amino groups at positions 3 and 6 become nucleophilic and prone to acylation in the presence of unreacted aryloyl chlorides. Therefore, coupling with sluggishly reactive amines (e.g., compound **12** and other aromatic amines) is limited to *N,N,N′,N′*-tetralkylrhodamines (rhodamine B, 101, TMR, etc.). Monoalkylated rhodamines were coupled with highly nucleophilic primary amines, such as methyl 3-aminopropionate or ethanolamine, using HATU or TSTU, which are two uronium peptide coupling reagents. Compounds **1** and **7** were prepared in this way (Scheme 2).

An alternative and simpler amidation protocol is based on the direct reaction of an alkyl ester of the rhodamine with a highly reactive primary amine in DMF at room temperature (or under gentle heating). Reaction yields are high enough (>60%),[39] but decrease when the hydrophilicity of the products increases. This approach is particularly advantageous for preparing derivatives of rhodamine 6G (e.g., compound **9**-alkyl), because this rhodamine is an ethyl ester. Other *N,N*-dialkylated rhodamines, such as rhodamine B, can be esterified by heating at reflux in ethanol with catalytic amounts of sulfuric acid, and then amidated. Some derivatives of compound **8** (Scheme 1) were prepared by this route.[20]

5.2 Functionalization and Labelling of the Target Molecules

A natural sequence of events (in most sample preparation protocols for fluorescence microscopies) consists of selecting the marker with required photophysical properties, designing and preparing a reactive compound (usually for coupling with amino or thiol groups, or for click chemistry), and, finally, labelling the structure or biomolecule of interest (e.g., protein, DNA, etc.) to perform the measurements. Two critical aspects for the success of this approach are the labelling efficiency that can be obtained (i.e., the number of target molecules labelled or the average number of markers per target) and the ability of the probe to retain its properties. Standard fluorescent markers usually lose part of the emission efficiency after coupling due to aggregation or quenching by possible proximal acceptors. In extreme cases, aggregation or precipitation of the labelled biomolecules (e.g., antibody) may occur. Common strategies to minimize this effect are the use of longer linkers (between the target and the probe) and the addition of hydrophilic groups.

Probes for stochastic nanoscopies should, additionally, retain the switching ability. The latter is an important factor, particularly for photochromic compounds. Many of them perform well in non-polar solvents and alcohols, but very poorly in aqueous solutions in which bleaching processes may efficiently compete with photochromism. The absence of the zwitterionic character makes an RSA less water soluble than its rhodamine counterpart. Moreover, the substituents introduced for tuning the absorp-

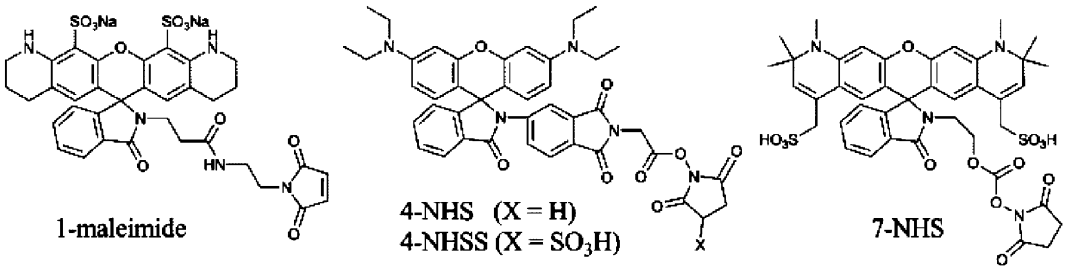

Scheme 3. Some amino- and thiol-reactive analogues of RSA.

tion and emission wavelengths tend to reduce the hydrophilicity even further. We addressed this problem using similar strategies to those described above. For example, sulfonic acid groups were introduced directly to the chromophore in compounds **1** and **7** to make them water soluble. In other cases, an *N*-hydroxy(sulfosuccinimidyl) (NHSS) ester was used as an amino-reactive moiety (compounds **2**–**6**),[16,17,25,32,40] when coupling was performed in aqueous buffered solutions. Nevertheless, even hydrophilic NHSS esters of compounds **2**, **3** and **6** provided low labelling efficiencies and poor long-term stability of the antibodies (because their dye residues are very lipophilic). However, they showed excellent performance in other applications, for example, an NHS derivative of compound **3** was coupled with (3-aminopropyl)triethoxysilane (APTES) and used in the preparation of silica nanoparticles that were imaged with high quality and resolution. The length of the linker was also selected to obtain bright adducts and reliable conjugation, for example, 3-aminopropionic acid residues were introduced between the probe and the reactive group (**1**, **1**-maleimide and analogues of compound **7**).

So far, two kinds of reactive probes have been prepared, amino-reactive NHS (NHSS) esters (**4**-NHS, **4**-NHSS) and NHS carbonate (**7**-NHS), as well as thiol-reactive maleimide (Scheme 3), and employed with standard protocols.[16] In all cases, the functional group was added in a post-synthetic modification of the previously prepared RSA (Scheme 2). An advantage of this approach is that two different reactive adducts can be freshly prepared before the labelling procedure from the same stock of the dye selected, which is chemically stable for long periods of time. As mentioned above, *N*-monoalkylated rhodamines are nucleophilic enough to react with an NHS ester, even when they are sterically hindered. When a solution of compound **1**-NHS (Scheme 2; R = *N*-hydroxysuccinimidyl) was prepared in DMF, a greenish tar was obtained within hours at 0°. Fortunately, we were able to isolate compound **1**-NHS, if the reaction was carried out quickly at 0° without an excess of base (Et_3N), the solvent (DMF) was removed in high vacuum at room temperature and the product was isolated by preparative HPLC in the presence of 0.1% TFA in the eluent. However, the stability of **1**-NHS was limited. Alternatively, thiol-reactive derivatives were used for protein labelling, rendering good-quality images.[17,25,37,41] For this, some of the terminal amino groups in antibodies were randomly modified with Traut's reagent and converted into thiol groups.

The commercially available RSA Abberior™ FLIP565 is also presented in Scheme 2.[42] It has the same core as that in compounds **4**-NHS and **4**-NHSS in Scheme 3. However, some new features were introduced. Tetramethylrhodamine (TMR) was used instead of rhodamine B and four CH_2 groups were "saved" (atom economy). Then, a special "hydrophilizer" was developed and introduced between the core and *N*-hydroxysuccinimidyl group. This modification provided good solubility in aqueous buffers, and a relatively stable NHS ester, which can be stored and shipped in a dry state.

6 Super-resolution Imaging with RSAs

6.1 Spatial Resolution

The localization accuracy ($\Delta x,y$) of SMs, and thus, the maximal spatial resolution that can be achieved with methods based on switching and localizing single emitters, depend on four factors, according to Equation (1).[9] The pixel size, a, and the standard deviation of the PSF, s, are fixed by instrumental conditions (numerical aperture of the objective lens and a combination of the physical size of the pixels of the CCD with the detection imaging system). The background noise, b, depends on the nature of the sample and the contribution from the signal coming from the markers in the dark isomer. As stated before, assuming that the first two parameters are properly selected and optimized, and the background noise can be kept low, $\Delta x,y$ depends only on the number of the detected photons (N_{PH}).

$$\Delta x, y = \sqrt{\frac{s^2}{N_{PH}} + \frac{a^2}{12N_{PH}} + \frac{4\sqrt{\pi s^2 b^2}}{a(N_{PH})^2}} \approx \sqrt{\frac{s^2}{N_{PH}}} \quad (1)$$

This value depends, in turn, on the brightness ($\varepsilon_{\lambda-EX}$-Φ_{Fluo}) of the marker in the emissive form, but it also strongly depends on the environment of every marker

and imaging conditions (excitation intensity, emission filters, etc.). Besides the known absorption coefficient at the excitation wavelength ($\varepsilon_{\lambda-EX}$) and the emission quantum yield (Φ_{Fluo}) in solution, a measurement of N_{PH} under standard imaging conditions is very useful for practical reasons. This value also correlates with the photostability of the fluorophore and depends on the triplet yield. N_{PH} is obtained for every imaging experiment and varies for the same marker from sample to sample. For comparison between the prepared RSAs, measurements in PVA films were undertaken (Table 1). PVA was used to fix the molecules and selected because it is one of the main components of Mowiol; a popular mounting medium for immunofluorescence experiments. Results indicated that spatial resolutions below 10–15 nm could be achieved. Such high values allow speeding up measurements (ca. 5-fold) with little sacrifice in localization accuracy.[16]

Table 1. Average photons per molecule in a 10 ms frame ($<N_{PH}>$) in PVA films observed in a wide-field microscope, under identical excitation intensities (532 nm), near the saturation values. Spectroscopic properties in aqueous solutions are also given. (Adapted with permission from reference [25].)

Compound	$\langle N_{PH}\rangle$ [a]	λ_{MAX} [nm]		τ [ns]
		CI (abs)	OI (abs/em)	OI
1	1600	331	537/555	4.1
2	1050	295	510/534	3.9
3	2350	301	536/557	–
4	1600	314	566/589	1.3
5	1350	338	596/618	3.5
6	1000	307	607/625	–
7	850	340	591/620	3.7

[a] Averaged from over 20000 SMs.

A more accurate value may be obtained in similar experiments using, for example, a labelled biomolecule. This could help to optimize the labelling efficiencies; then the $\langle N_{PH}\rangle$ value can eventually be adjusted by changing the marker/target ratio in the staining protocol.

6.2 One Colour and Multicolour Imaging

Reactive derivatives of compounds **1**–**7** (Scheme 1) have been used for labelling proteins,[40] aptamers,[41] or secondary antibodies for standard immunostaining,[16,17,25] as well as polymers[18] or silica gel (nano)particles.[16,17,32,43] For example, tubulin filaments have been observed with sizes between 55 and 70 nm (Figure 5), which is close to the theoretical value expected if the sizes of the filament and the primary and secondary antibodies are taken into account. These results indicate that resolution has been improved to the point where labelling strategies become one of the limiting factors.[10] Direct labelling with RSAs bypasses that problem. This approach was applied to the study of amyloid aggregation of α-synuclein (AS), a small 15 kDa protein engaged in the progress of Parkinson's disease. Super-resolution imaging revealed intracellular aggregates with average sizes below 40 nm in diameter, and allowed an estimation of the number of monomeric proteins in those minute structures. Moreover, the average diameter of *in vitro* fibrillar structures (24 nm; Figure 6A) was in accordance with AFM measurements.

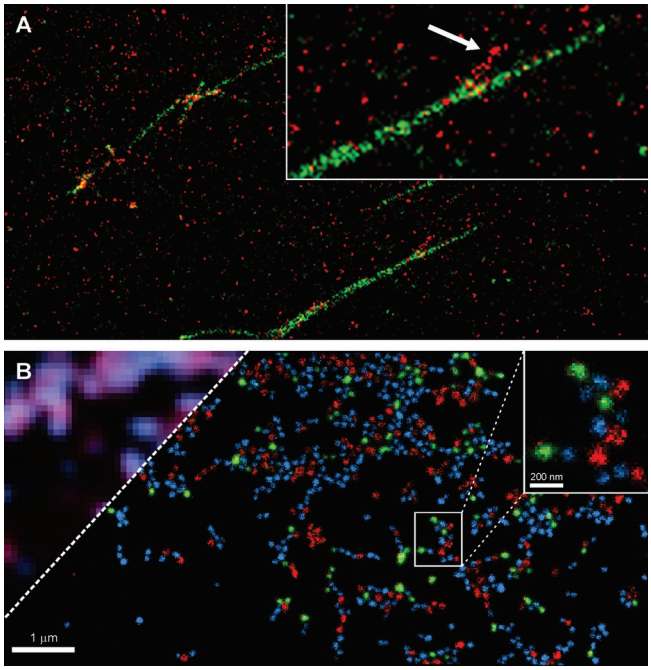

Figure 6. Multicolour super-resolution imaging with RSAs. A) *In vitro* elongation of AS fibrils. Fibrils were first formed with AS with a green RSA marker and then incubated with AS with a red RSA marker. The arrow shows elongation from a branching point. B) Three kinds of silica nanoparticles, each with a different RSA, were imaged and separation of markers with different emission wavelengths at the sub-diffraction level in a two-channel detection setup was achieved. (Adapted with permission from references [17] and [40].)

Two-colour experiments revealed a unidirectional elongation of single fibrils at an average rate of 7 nm min^{-1}, starting from the fibril tip or from a branching point.

Multicolour imaging of RSAs was performed with an imaging approach, relying on the spectral properties of each single emitter.[17,44] A major advantage of such a method is that, unlike in ensemble measurements of standard diffraction-limited microscopies, it is not necessary that the number of detection channels matches or exceeds that of the imaged species (e.g., with different emission colours). This was proved first with a mixture of three kinds of silica gel nanoparticles, labelled with various RSAs. A sharp three-colour separation with sub-diffraction resolution was achieved with only two detection channels (Figure 6B). The high cost of the detectors for SMs makes this advantage important for the setup design.

Moreover, the three RSAs required only two laser sources, for photoswitching and excitation.

An additional advantage of imaging with RSAs is that total recording times are in the order of a few minutes, due to their photophysical (photoswitching and emission) properties and their use in combination with a fast and asynchronous image acquisition protocol.[23] Unlike other probes, RSAs do not require a laser dedicated for switching off or a delay to compensate for a slow thermal recovery and are perfectly suitable for asynchronous frame acquisition at fast (2–20 ms)[16] frame exposure times. In such recording schemes, the exposure time is matched to the average "on" time of the marker (average time spent in the emissive isomer). The lifetime of the OI varies with the RSA and environment, and thus, frame rates have to be adjusted for each particular case. The excitation intensity was also found to play a role, since there was a competition between two switching-off processes: the thermal back conversion discussed above and photobleaching to a non-emissive product. This is probably a common phenomenon that applies to most molecular photoswitches, irrespective of their switching mechanism, considering the harsh excitation conditions required for SM detection.

6.3 Optical Sectioning and 3D Super-resolution

One of the common problems in SM detection is the background signal [*b*, Eq. (1)]. The spatial resolution can be seriously limited if this background signal cannot be reduced, even if very effective markers are used. The factors contributing to the background vary with each particular sample; possible reasons are sample scattering and autofluorescence. Common strategies to reduce this signal are the use of cryosectioned thin samples or total internal reflection fluorescence (TIRF) illumination, which limits the penetration of light to a depth of about 100 nm. Clear disadvantages are incompatibility with live-

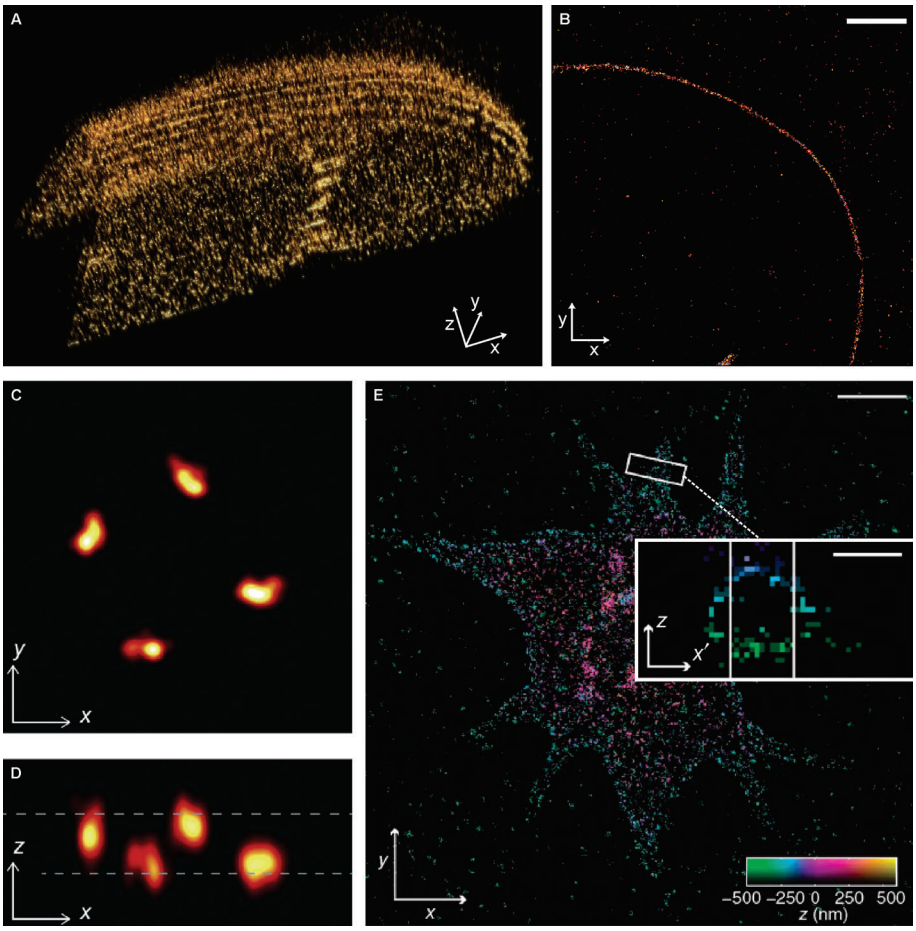

Figure 7. 3D super-resolution with optical sectioning achieved by two-photon activation of compound **4**-NHSS (coupled to a secondary antibody). A) 3D reconstruction of a U373 MG cell (10 *z*-slices). B) The equatorial slice is shown (scale bar, 2 μm). 3D super-resolution imaging with astigmatic (C,D) or interferometric (E) detection schemes. Imaging single poly(butyl methacrylate) (PBMA) chains labelled with RSA in a 210 nm thick film (arrow size, 200 nm). E) Image of receptor GPIIb/IIIa in a human platelet by immunolabelling with compound **1**-maleimide; the colour encodes the axial position of each marker (scale bar, 1 μm). The inset shows an *x*–*z* projection of the boxed region (scale bar, 200 nm). (Adapted with permission from references [16], [18] and [37].)

cell imaging and more complicated sample preparation (in the first case), as well as the limitation of observation to the thin layer in contact with the substrate. The possibility to switch RSAs through a two-photon absorption process is an alternative that helps to circumvent the problem. Although the contribution produced by excitation light is not excluded, long wavelengths produce less scattering than UV light and have less chance to excite intrinsic fluorescent species, in addition to deeper penetration and the fact that they are almost harmless to live species. *Z* stacks recorded in whole thick samples (e.g., whole fixed cells) proved the advantages of two-photon activation (Figure 7A and B). High-resolution images at a depth of several microns are impossible with a one-photon absorption process.

The conformation of single PBMA chains with an RSA marker was investigated with 3D super-resolution by Ito et al.[18] A methacrylate monomer with an RSA moiety (compound **8** in Scheme 1; $R=(CH_2)_2OH$) was synthesized by esterification with methacryloyl chloride. The copolymer was prepared by atom-transfer radical copolymerization of mixtures of butyl methacrylate and the labelled monomer. Interestingly, the RSA survived the reaction conditions and, in the amount used (a fraction below 1%), it did not alter the properties of the polymer. Resolution down to 15 nm was achieved with the aid of 100 nm gold beads as fiduciary markers for drift compensation. Astigmatic imaging revealed the 3D structure of individual chains (Figure 7C and D); a random coil conformation was concluded from the direct observation of individual PBMA in a bulk film.

3D super-resolution imaging with RSA was also performed in a setup with an interferometric (4PI)[45] detection scheme.[37] By taking advantage of an increase in the total numerical aperture, resulting from the use of two opposing high numerical aperture (NA) objective lenses, a localization precision below 10 nm in all three directions was possible in a thick layer ($\approx$650 nm) that could be at an arbitrarily selected depth in the sample. The glycoprotein IIb/IIIa receptor on human platelets immunostained with a secondary antibody labelled with compound **1**-maleimide was observed in such a setup (Figure 7E). The impressive resolution obtained was one of the best currently achievable with a SM localization technique and superior to any other single-lens detection method.

7 Conclusion

Far-field fluorescence microscopy has recently improved its resolution power from hundreds to a few nanometres. These exciting changes were only possible with fluorescent markers, the signal of which could be photoswitched between bright and dark states. Photochromic synthetic compounds have played an important role in this process and contributed greatly RSAs. Robust fluorescent properties, reliable photoactivation, and relatively easy chemistry are some of the advantages that led to them being versatile markers for diverse applications. This remarkable family of compounds, combined with the chemical design of the molecular systems, provided short recording times, simple multicolour imaging, and optical sectioning.

All of the examples discussed above share a common feature: a notable resolution enhancement that allows the observation of objects or structures that are otherwise impossible to discern in classical wide-field microscopes. The photoswitching of the emission signal of RSAs clearly fulfils the demanding requirements of the stochastic imaging scheme based on the localization of single emitters.

Fluorescence nanoscopies will surely expand in coming years and molecular photoswitches will have to evolve and be developed to accompany and encompass these changes. One representative of RSAs, Abberior FLIP 565, is now commercially available,[42] but nonetheless this family of markers can profit from further improvements. In particular, an increase in their hydrophilic character and water solubility has to be achieved to broaden their range of utility in biological applications.

Acknowledgements

V. N. B. is indebted to the Max Planck Institute for Biophysical Chemistry (Göttingen, Germany) and to Prof. S. W. Hell (Head of NanoBiophotonics Dep.) for excellent research facilities. M. L. B. is a member of the research staff at CONICET (Miembro de la carrera del investigador científico del Consejo Nacional de Investigaciones Científicas y Técnicas, Argentina). This work was performed with support from UBA and ANPCyT (Argentina), and the Max Planck Society (Germany) through a Partner Group Grant. M. L. B. is indebted to Prof. S. W. Hell for constant support. We are grateful to J. Jethwa for proof-reading the manuscript.

References

[1] a) S. W. Hell, J. Wichmann, *Opt. Lett.* **1994**, *19*, 780–782; b) S. W. Hell, *Nat. Biotechnol.* **2003**, *21*, 1347–1355; c) S. W. Hell, *Phys. Lett. A* **2004**, *326*, 140–145; d) S. W. Hell, *Science* **2007**, *316*, 1153–1158; e) S. W. Hell, *Nat. Methods* **2009**, *6*, 24–32.

[2] M. Hofmann, C. Eggeling, S. Jakobs, S. W. Hell, *Proc. Natl. Acad. Sci. USA* **2005**, *102*, 17565–17569; b) M. L. Bossi, J. Fölling, M. Dyba, V. Westphal, S. W. Hell, *New J. Phys.* **2006**, *8*, 275.

[3] E. Betzig, G. H. Patterson, R. Sougrat, O. Wolf Lindwasser, S. Olenych, J. S. Bonifacino, M. W. Davidson, J. Lippincott-Schwartz, H. F. Hess, *Science* **2006**, *313*, 1642–1645.

[4] M. J. Rust, M. Bates, X. Zhuang, *Nat. Methods* **2006**, *3*, 793–796.

[5] J. Fölling, M. Bossi, H. Bock, R. Medda, C. A. Wurm, B. Hein, S. Jakobs, C. Eggeling, S. W. Hell, *Nat. Methods* **2008**, *5*, 943–945.
[6] a) R. Heintzmann, T. M. Jovin, C. Cremer, *J. Opt. Soc. Am. A* **2002**, *19*, 1599–1609; b) M. G. L. Gustafsson, *Proc. Natl. Acad. Sci. USA* **2005**, *102*, 13081–13086; c) S. Bretschneider, C. Eggeling, S. W. Hell, *Phys. Rev. Lett.* **2007**, *98*, 218103.
[7] S. T. Hess, T. P. K. Girirajan, M. D. Mason, *Biophys. J.* **2006**, *91*, 4258–4272; b) A. Sharonov, R. M. Hochstrasser, *Proc. Natl. Acad. Sci. USA* **2006**, *103*, 18911–18916; c) M. Heilemann, S. van de Linde, M. Schüttpelz, R. Kasper, B. Seefeldt, A. Mukherjee, P. Tinnefeld, M. Sauer, *Angew. Chem. Int. Ed.* **2008**, *47*, 6172–6176.
[8] B. Huang, M. Bates, X. Zhuang, *Annu. Rev. Biochem.* **2009**, *78*, 993–1016.
[9] R. E. Thompson, D. R. Larson, W. W. Webb, *Biophys. J.* **2002**, *82*, 2775–2783.
[10] a) M. Fernández-Suárez, A. Y. Ting, *Nat. Rev. Mol. Cell Biol.* **2008**, *9*, 929–943; b) M. Heilemann, P. Dedecker, J. Hofkens, M. Sauer, *Laser Photonics Rev.* **2009**, *3*, 180–202; c) J. Vogelsang, C. Steinhauer, C. Forthmann, I. H. Stein, B. Person-Skegro, T. Cordes, P. Tinnefeld, *ChemPhysChem* **2010**, *11*, 2475–2490; d) F. M. Raymo, *J. Phys. Chem. Lett.* **2012**, *3*, 2379–2385.
[11] F. M. Raymo, M. Tomasulo, *Chem. Soc. Rev.* **2005**, *34*, 327–336.
[12] a) M. Irie, T. Fukaminato, T. Sasaki, N. Tamai, T. Kawai, *Nature* **2002**, *420*, 759–760; b) T. Fukaminato, T. Umemoto, Y. Iwata, S. Yokojima, M. Yoneyama, S. Nakamura, M. Irie, *J. Am. Chem. Soc.* **2007**, *129*, 5932–5938; c) T. Fukaminato, T. Doi, N. Tamaoki, K. Okuno, Y. Ishibashi, H. Miyasaka, M. Irie, *J. Am. Chem. Soc.* **2011**, *133*, 4984–4990; M. Irie, *Photochem. Photobiol. Sci.* **2010**, *9*, 1535–1542.
[13] L. Giordano, T. M. Jovin, M. Irie, E. A. Jares-Erijman, *J. Am. Chem. Soc.* **2002**, *124*, 7481–7489.
[14] T. Fukaminato, T. Sasaki, T. Kawai, N. Tamai, M. Irie, *J. Am. Chem. Soc.* **2004**, *126*, 14843–14849.
[15] a) E. Deniz, S. Sortino, F. M. Raymo, *J. Phys. Chem. Lett.* **2010**, *1*, 3506–3509; b) E. Deniz, M. Tomasulo, J. Cusido, S. Sortino, F. M. Raymo, *Langmuir* **2011**, *27*, 11773–11783; c) E. Deniz, M. Tomasulo, J. Cusido, I. Yildiz, M. Petriella, M. L. Bossi, S. Sortino, F. M. Raymo, *J. Phys. Chem. C* **2012**, *116*, 6058–6068.
[16] J. Föling, V. Belov, R. Kunetsky, R. Medda, A. Schönle, A. Egner, C. Eggeling, M. Bossi, S. W. Hell, *Angew. Chem. Int. Ed.* **2007**, *46*, 6266–6270.
[17] M. Bossi, J. Fölling, V. N. Belov, V. P. Boyarskiy, R. Medda, A. Egner, C. Eggeling, A. Schönle, S. W. Hell, *Nano Lett.* **2008**, *8*, 2463–2468.
[18] H. Aoki, K. Morib, S. Ito, *Soft Matter* **2012**, *8*, 4390–4395.
[19] a) K. H. Knauer, R. Gleiter, *Angew. Chem. Int. Ed. Engl.* **1977**, *16*, 113–113; b) H. Willwohl, J. Wolfrum, R. Gleiter, *Laser Chem.* **1989**, *10*, 63–72.
[20] H. Montenegro, M. Di Paolo, D. Capdevila, P. F. Aramendía, M. L. Bossi, *Photochem. Photobiol. Sci.* **2012**, *11*, 1081–1086.
[21] H. Bouas-Laurent, H. Dürr, *Pure Appl. Chem.* **2001**, *73*, 639–665.
[22] a) S. Kummer, R. M. Dickson, W. E. Moerner, *Proc. SPIE* **1998**, *3273*, 165–173; b) R. Zondervan, F. Kulzer, S. B. Orlinskii, M. Orrit, *J. Phys. Chem. A* **2003**, *107*, 6770–6776.
[23] C. Geisler, A. Schönle, C. v. Middendorff, H. Bock, C. Eggeling, A. Egner, S. W. Hell, *Appl. Phys. A* **2007**, *88*, 223–226; b) A. Egner, C. Geisler, C. v. Middendorff, H. Bock, D. Wenzel, R. Medda, M. Andresen, A. C. Stiel, S. Jakobs, C. Eggeling, A. Schönle, S. W. Hell, *Biophys. J.* **2007**, *93*, 3285–3290.
[24] Recently, a RSA with reverse behaviour was introduced: H. Li, H. Guan, X. Duan, J. Hu, G. Wang, Q. Wang, *Org. Biomol. Chem.* **2013**, *11*, 1805-1809.
[25] V. N. Belov, M. L. Bossi, J. Fölling, V. P. Boyarskiy, S. W. Hell, *Chem. Eur. J.* **2009**, *15*, 10762–10776.
[26] a) H. Kim, M. Lee, H. Kim, J. Kim, J. Yoon, *Chem. Soc. Rev.* **2008**, *37*, 1465–1472; b) X. Chen, T. Pradhan, F. Wang, J. S. Kim, J. Yoon, *Chem. Rev.* **2012**, *112*, 1910–1956.
[27] L. Wu, Y. Dai, G. Marriott, *Org. Lett.* **2011**, *13*, 2018–2021.
[28] T. Nguyen, M. B. Francis, *Org. Lett.* **2003**, *5*, 3245–3248.
[29] M. Bossi, V. Belov, S. Polyakova, S. W. Hell, *Angew. Chem. Int. Ed.* **2006**, *45*, 7462–7465.
[30] See, for example, www.atto-tec.com.
[31] V. P. Boyarskiy, V. N. Belov, R. Medda, B. Hein, M. Bossi, S. W. Hell, *Chem. Eur. J.* **2008**, *14*,1784–1792.
[32] J. Fölling, V. Belov, D. Riedel, A. Schönle, A. Egner, C. Eggeling, M. Bossi, S. W. Hell, *ChemPhysChem* **2008**, *9*, 321–326.
[33] W. R. Zipfel, R. M. Williams, W. W. Webb, *Nat. Biotechnol.* **2003**, *21*, 1369–1377.
[34] B. Huang, W. Wang, M. Bates, X. Zhuang, *Science* **2008**, *319*, 810–813.
[35] M. F. Juette, T. J. Gould, M. D. Lessard, M. J. Mlodzianoski, B. S. Nagpure, B. T. Bennett, S. T. Hess, J. Bewersdorf, *Nat. Methods* **2008**, *5*, 527–529.
[36] a) G. Shtengel, J. A. Galbraith, C. G. Galbraith, J. Lippincott-Schwartz, J. M. Gillette, S. Manley, R. Sougrat, C. M. Waterman, P. Kanchanawong, M. W. Davidson, R. D. Fetter, H. F. Hess, *Proc. Natl. Acad. Sci. USA* **2009**, *106*, 3125–3130.
[37] D. Aquino, A. Schönle, C. Geisler, C. v. Middendorff, C. A. Wurm, Y. Okamura, T. Lang, S. W. Hell, A. Egner, *Nat. Methods* **2011**, *8*, 353–359.
[38] V. N. Belov, C. A. Wurm, V. P. Boyarskiy, S. Jakobs, S. W. Hell, *Angew. Chem. Int. Ed.* **2010**, *49*, 3520–3523.
[39] a) M. Adamczyk, J. Grote, *Bioorg. Med. Chem. Lett.* **2000**, *10*, 1539–1541; b) M. Adamczyk, J. Grote, *Bioorg. Med. Chem. Lett.* **2003**, *13*, 2327–2330.
[40] M. J. Roberti, J. Fölling, M. S. Celej, M. Bossi, T. M. Jovin, E. A. Jares-Erijman, *Biophys. J.* **2012**, *102*, 1598–1607.
[41] F. Opazo, M. Levy, M. Byrom, C. Schäfer, C. Geisler, T. W. Groemer, A. D. Ellington, S. O. Rizzoli, *Nat. Methods* **2012**, *9*, 938–939.
[42] www.abberior.com.
[43] I. Testa, A. Schönle, C. v. Middendorff, C. Geisler, R. Medda, C. A. Wurm, A. C. Stiel, S. Jakobs, M. Bossi, C. Eggeling, S. W. Hell, A. Egner, *Opt. Express* **2008**, *16*, 21093–21104.
[44] A. Schönle, S. W. Hell, *Nat. Biotechnol.* **2007**, *25*, 1234–1235.
[45] S. W. Hell, E. H. K. Stelzer, *J. Opt. Soc. Am. A* **1992**, *9*, 2159–2166.

Received: February 14, 2013
Accepted: March 23, 2013
Published online: May 9, 2013

